Marine and Petroleum Geology 75 (2016) 140–150

Contents lists available at ScienceDirect

Marine and Petroleum Geology

journal homepage: www.elsevier.com/locate/marpetgeo

Research paper

Sedimentary and residual gas geochemical characteristics of the Lower Cambrian organic-rich shales in Southeastern Chongqing, China

Chenjun Wu [a], Jincai Tuo [a, *], Mingfeng Zhang [a], Lina Sun [a, b], Yu Qian [a, b], Yan Liu [a]

[a] Key Laboratory of Petroleum Resources, Gansu Province/Key Laboratory of Petroleum Resources Research, Institute of Geology and Geophysics, Chinese Academy of Sciences, Lanzhou 730000, China
[b] University of Chinese Academy of Sciences, Beijing 100049, China

ARTICLE INFO

Article history:
Received 25 November 2015
Received in revised form
12 April 2016
Accepted 18 April 2016
Available online 20 April 2016

Keywords:
Niutitang formation
Organic-rich shales
Sedimentary environment
Residual gas

ABSTRACT

To study the sedimentary environment of the Lower Cambrian organic-rich shales and isotopic geochemical characteristics of the residual shale gas, 20 black shale samples from the Niutitang Formation were collected from the Youyang section, located in southeastern Chongqing, China. A combination of geochemical, mineralogical, and trace element studies has been performed on the shale samples from the Lower Cambrian Niutitang Formation, and the results were used to determine the paleoceanic sedimentary environment of this organic-rich shale. The relationships between total organic carbon (TOC) and total sulfur (TS) content, carbon isotope value ($\delta^{13}C_{org}$), trace element enrichment, and mineral composition suggest that the high-TOC Niutitang shale was deposited in an anoxic environment and that the organic matter was well preserved after burial. Stable carbon isotopes and biomarkers both indicate that the organic matter in the Niutitang black shales was mainly derived from both lower aquatic organisms and algaes and belong to type I kerogen. The oil-prone Niutitang black shales have limited residual hydrocarbons, with low values of S_2, I_H, and bitumen A. The carbon isotopic distribution of the residual gas indicate that the shale gas stored in the Niutitang black shale was mostly generated from the cracking of residual bitumen and wet gas during a stage of significantly high maturity. One of the more significant observations in this work involves the carbon isotope compositions of the residual gas (C_1, C_2, and C_3) released by rock crushing. A conventional $\delta^{13}C_1$–$\delta^{13}C_2$ trend was observed, and most $\delta^{13}C_2$ values of the residual gases are heavier than those of the organic matter (OM) in the corresponding samples, indicating the splitting of ethane bonds and the release of smaller molecules, leading to ^{13}C enrichment in the residual ethane.

1. Introduction

The increasing global demand for clean energy has made it imperative to search for and exploit unconventional oil and gas resources. Organic-rich shales have received renewed attention because of their emergence as unconventional hydrocarbon reservoirs (Jarvie et al., 2007; Loucks and Ruppel, 2007). In recent years, upper Yangtze Region in southern China has become the leading area for exploration and development of shale gas in China (Tian et al., 2013; Dai et al., 2014; Zou et al., 2015). Marine black shales were widely developed during the Early Cambrian (Niutitang Formation, also called the Qiongzhusi Formation or Jiulaodong Formation in the southwestern part of the Sichuan Basin), Late Ordovician (Wufeng Formation), and Early Silurian (Longmaxi Formation) periods (Zhang et al., 2008; Zou and Dong, 2010, 2015; Hao et al., 2013). The Wufeng-Longmaxi Formation in south China as potential shale gas strata has been studied for several years. Discovery of the Jiaoshiba shale gas field in southeastern margin of the Sichuan Basin marks a significant progress in the shale gas exploration in the Wufeng-Longmaxi Formation and has a guiding significance for shale gas exploration and development in China (Guo and Zhang, 2014). From 2012 to July 2015, the Jiaoshiba shale gas field has produced shale gas about 21.24×10^8 m^3 with daily shale gas production up to 1200×10^4 m^3/day (Chen et al., 2015). Compared with the Upper Ordovician-Lower Silurian shales, the Lower Cambrian Niutitang shales are more widely and stably distributed throughout southern China, and contain higher TOC with greater thermal maturity levels (Wang et al., 2014a,b; Tian

* Corresponding author.
E-mail address: jctuo@ns.lzb.ac.cn (J. Tuo).

http://dx.doi.org/10.1016/j.marpetgeo.2016.04.013
0264-8172/

et al., 2015; Zou et al., 2015). Therefore, the Lower Cambrian black shales also have a promising potential of shale gas.

Stable carbon isotope study of residual gas in shales that can be recovered with rock crushing provides useful information for identifying the origin of shale gas. Zhang et al. (2014) studied gas geochemical characteristics of the residual gas from Barnett shales. The chemical and carbon isotopic compositions of crushed-rock gases from organic-rich Barnett shale core samples with a wide range of thermal maturities (0.58–2.07%R_o) were analyzed and compared to previously reported the chemical and isotopic compositions of produced gas from Barnett Shale, providing information of great relevance for understanding deep shale gas reservoirs. Tang et al. (2015) analyzed the chemical and carbon isotopic compositions of residual gas in organic-rich Longmaxi shales. The $\delta^{13}C$ values of C_1, C_2, C_3, and CO_2 of residual gas have similar features to the produced gas from the weiyuan shale-gas play, providing important evidence of the origin and storage of shale gas in organic-rich Longmaxi shales.

In this study, the geochemistry and carbon isotopic characteristic of the Lower Cambrian Niutitang organic-rich shales and their residual gases are investigated. The main objectives of this study are to investigate (1) the sedimentary environment of the Lower Cambrian organic-rich shales, (2) the carbon isotopic distribution of the residual gas released by the method of rock crushing, and (3) the genetic origin of shale gas in the Lower Cambrian shales.

2. Geological setting

The Upper Yangtze Platform tectonically comprises the western part of the Yangtze Platform in South China. It regionally includes the eastern Sichuan, Chongqing area, most of Guizhou, western Hubei and Hunan, and northern Yunnan province (Tan et al., 2013). A major marine transgression occurred in the early Cambrian in this region, causing thick black shale extensively deposited in restricted marine environments. During the Early Cambrian, the whole Upper Yangtze Platform could be considered a pericontinental marine shelf. The paleocontinent was located in the west, and the depositional environments gradually changed to a marine platform, restricted marine basin, former island arc system, and deep marine setting toward the southeast (Tan et al., 2014, 2015). The Lower Cambrian black shales were recognized as one of the major source rocks in the Upper Yangtze Platform. Southeastern Chongqing, geographically located in eastern Sichuan Basin and tectonically situated in the transitional zone between the middle part of the Central Sichuan Uplift and the Central Guizhou Uplift, is an important part of the Upper Yangtze plate. The strata in this area are mainly Cambrian, Ordovician, Silurian, Devonian, and Permian. Effected by tectonic uplift, other strata are missing. The Lower Silurian Longmaxi and Lower Cambrian Niutitang shales are the main hydrocarbon source rocks in this area. The discovery of the Jiaoshiba Longmaxi shale gas field, located in Jiaoshiba County, Fuling District of Chongqing, marks a breakthrough in shale gas exploration and development in southeastern Chongqing (Guo et al., 2007). The Lower Cambrian Niutitang shale is another main hydrocarbon source rock with promising shale gas potential in this area.

The organic-rich Niutitang shales are distributed throughout southeastern Chongqing, with a total thickness of greater than 100 m in most area of southeastern Chongqing and up to 180–200 m in Youyang and Xiushan areas. A set of high-quality shales is present in the lower part of the Niutitang Formation. Because of the Tongwan tectonic movement at the end of the Proterozoic, the Niutitang shales unconformable contact with the underlying dolomite in the upper Sinian Dengying Formation (Mei et al., 2006; Tan et al., 2014). The thickness of the organic-rich shales with a total organic carbon content greater than 2.0% ranges from 40 to 60 m (Fig. 1). This study focuses on the high-quality shale present in the lower part of the Niutitang Formation. The studied section is located in Tongling village (N28°38′57.39″, E108°52′41.33″), Youyang county, southeastern Chongqing area. The stratigraphy of the studied profile is the lower part of the Niutitang Formation. The outcrop thickness of the Youyang profile is 23 m, and the profile features siliceous shale and black shale.

3. Samples and analytical methods

3.1. Samples

Twenty Lower Cambrian Niutitang shale samples were collected with an interval of 1 m from the Youyang outcrop section. To avoid the possible effects of weathering on the nature of outcrop shales, only fresh samples were collected during mining (Fig. 1). All the twenty samples were analyzed for total organic carbon (TOC), total sulfur (TS), stable carbon isotope of kerogen ($\delta^{13}C_{org}$), Gas chromatography-mass spectrometry (GC-MS), and carbon isotope of residual gas. A total of 17 samples were chosen for trace elements analyses, and 9 samples for mineral composition studies. All the analyses were performed in Key Laboratory of Petroleum Resources Research, Institute of Geology and Geophysics, Chinese Academy of Sciences, China.

3.2. Organic geochemistry

TOC and TS were measured with a CS344 analyzer after the samples were treated with 10% hydrochloric acid to remove carbonate and the analysis precisions are ±0.5%. The carbon isotopes of organic matter ($\delta^{13}C_{org}$) were determined on shales after removing carbonate by an instrument of Thermo Fisher MAT-253-FLASH 2000 and reported in per mil (‰) relative to Peedee belemnite (PDB) standard with an analysis precision of ±0.3‰, using IAEA-600 caffeine as certified reference material (Coplen et al., 2006).

GC-MS analyses of soluble extracts were performed on a Hewlett-Packard 5890II gas chromatograph interfaced with a Hewlett-Packard 5989-A mass spectrometer. The mass spectrometer was operated at an electron energy of 70 eV and ion source temperature of 250 °C. The oven temperature was programmed to increase from 80 to 200 °C at 4 °C/min and then from 200 to 300 °C at 3 °C/min.

3.3. Trace elements and minerals

Trace elemental analyses were carried out using inductively coupled plasma-mass spectrometry (ICP-MS). The analytical uncertainties are estimated to be 5%. The standard rock reference materials were used to monitor the analytical accuracy and precision. Mineral composition were measured via Rigaku D/max-rA12KW rotating anode X-ray diffractometer 40 kV and 100 mA with a Cu Kα radiation. Stepwise scanning measurements were performed at a rate of 4°/min in the range of 3–85° (2θ).

3.4. Geochemistry of residual gas in shales

Residual gas in shales were recovered with a gas degasification-collection device that is modified from a prototype six-jar planetary high-energy ball mill device made by the Fritsch Company of Germany. By crushing samples using a ball mill, residual gas were collected in the absence of aqueous media under high vacuum conditions (Shi et al., 2012). Carbon isotopes of the recovered residual gases were analyzed by isotope mass spectrometer (DELTA plus XP) with an analysis precision of ±0.3%.

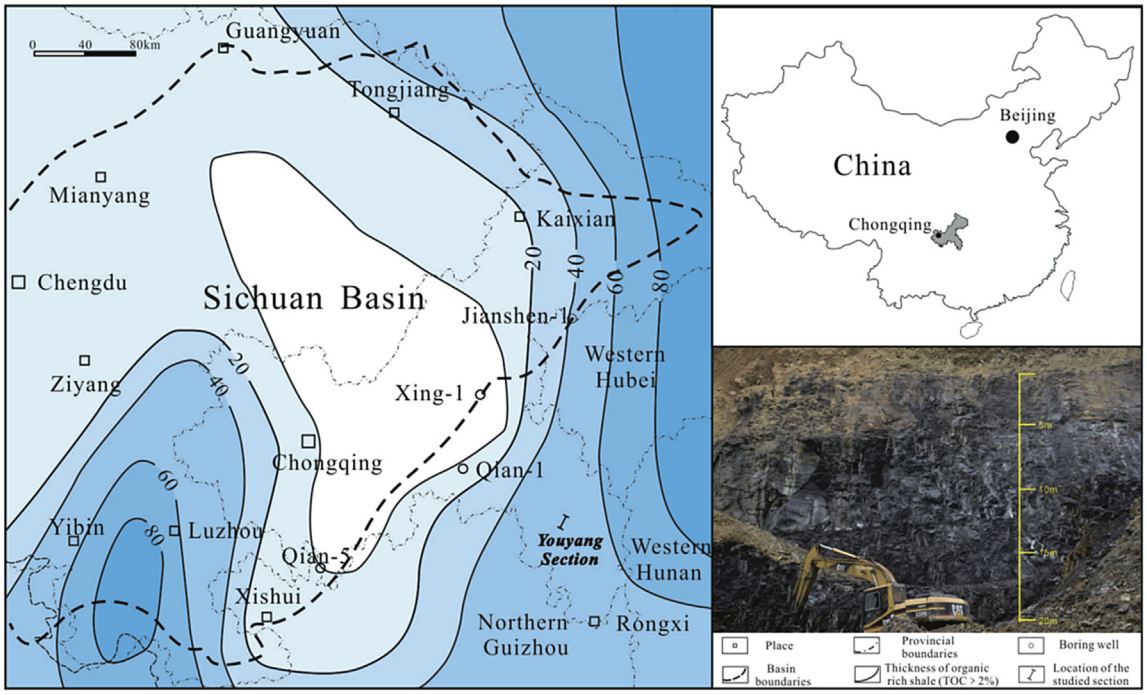

Fig. 1. Location and outcrop photograph of studied section in Southeastern Chongqing, China.

4. Results

4.1. TOC and TS

The twenty samples show relatively high TOC content ranging between 2.42% and 9.89%, with an average value of 7.0%; total sulfur content (TS) range between 0.15% and 5.3% with an average value of 3.6%. Both the TOC and TS content decreases upward (Table 1, Fig. 2).

4.2. Organic carbon isotopes

The carbon isotope ratios of organic matter concentrated from the Niutitang shales range between −32.4‰ and −31.1‰ with an average value of −31.8‰, exhibiting an obviously negative excursion in comparison with upper part of the Lower Cambrian Niutitang Formation (Wang et al., 2015) and a negative correlation with TOC contents (Fig. 2).

4.3. Biomarkers

Biomarker can provide important information about the organic matter source and redox conditions. However the abundance of extractable bitumen is extremely low if the organic matter has entered the highly mature to over-mature stages (Peters et al., 2005). Several studies suggested that possible contamination by

Table 1
Geochemical analysis results of the Niutitang black shales in Youyang Profile.

Sample no.	TOC (%)	S (%)	$\delta^{13}C_{org}$ (‰)	S_1 (mg/g)	S_2 (mg/g)	"A" (ppm)	$\sum nC_{21-}/\sum nC_{22+}$	Pr/C_{17}	Ph/C_{18}	Steranes (%)		
										$C_{27}R\alpha\alpha\alpha$	$C_{28}R\alpha\alpha\alpha$	$C_{29}R\alpha\alpha\alpha$
TL-1	3.39	0.15	−31.1	0.12	0.02	15.8	35.49	1.08	0.66	38.24	25.74	36.03
TL-2	2.42	0.24	−31.5	0.08	nd	13.1	65.20	1.08	0.60	35.77	26.83	37.40
TL-3	2.92	2.06	−31.6	0.08	nd	6.7	36.71	1.25	0.80	39.02	22.76	38.21
TL-4	3.59	2.02	−31.5	0.12	0.04	8.0	44.96	1.37	0.86	40.52	22.41	37.07
TL-5	8.42	4.78	−31.8	0.06	nd	9.1	18.17	1.46	0.69	41.32	19.01	39.67
TL-6	6.64	3.41	−31.6	0.08	nd	10.9	138.39	1.80	1.06	46.53	18.81	34.65
TL-7	6.92	3.69	−31.5	0.06	nd	6.8	61.83	1.65	1.11	48.62	16.51	34.86
TL-8	7.6	3.78	−31.8	0.10	nd	19.3	70.75	2.33	1.00	39.17	23.33	37.50
TL-9	7.31	4.35	−31.7	0.12	0.02	17.5	74.73	3.42	1.26	39.52	24.19	36.29
TL-10	8.02	5.23	−31.7	0.16	0.02	13.9	102.43	3.16	1.93	36.21	20.69	43.10
TL-11	7.95	4.17	−31.6	0.16	0.02	6.7	27.54	2.23	1.25	44.14	20.72	35.14
TL-12	8.27	4.92	−31.8	0.18	0.06	13.1	19.41	3.30	1.35	40.00	22.73	37.27
TL-13	8.92	5.05	−31.8	0.06	nd	14.7	7.49	8.52	3.62	36.15	25.38	38.46
TL-14	7.57	3.5	−31.7	0.07	0.01	14.2	40.64	3.01	1.40	40.91	20.91	38.18
TL-15	6.67	2.54	−31.6	0.04	0.01	8.8	19.28	2.01	0.98	42.86	20.17	36.97
TL-16	7.58	4.72	−31.6	0.07	0.01	10.4	16.05	3.33	1.53	41.44	22.52	36.04
TL-17	8.11	4.5	−31.7	0.06	0.01	9.9	23.50	3.41	1.77	39.29	22.32	38.39
TL-18	9.58	5.3	−32.0	0.05	nd	7.0	12.25	3.71	2.05	41.18	19.33	39.50
TL-19	9.89	3.83	−32.2	0.06	nd	9.6	42.26	2.83	1.27	42.20	22.02	35.78
TL-20	8.14	3.77	−31.9	0.06	nd	11.3	76.43	1.86	0.66	39.09	21.82	39.09

nd: no detected.

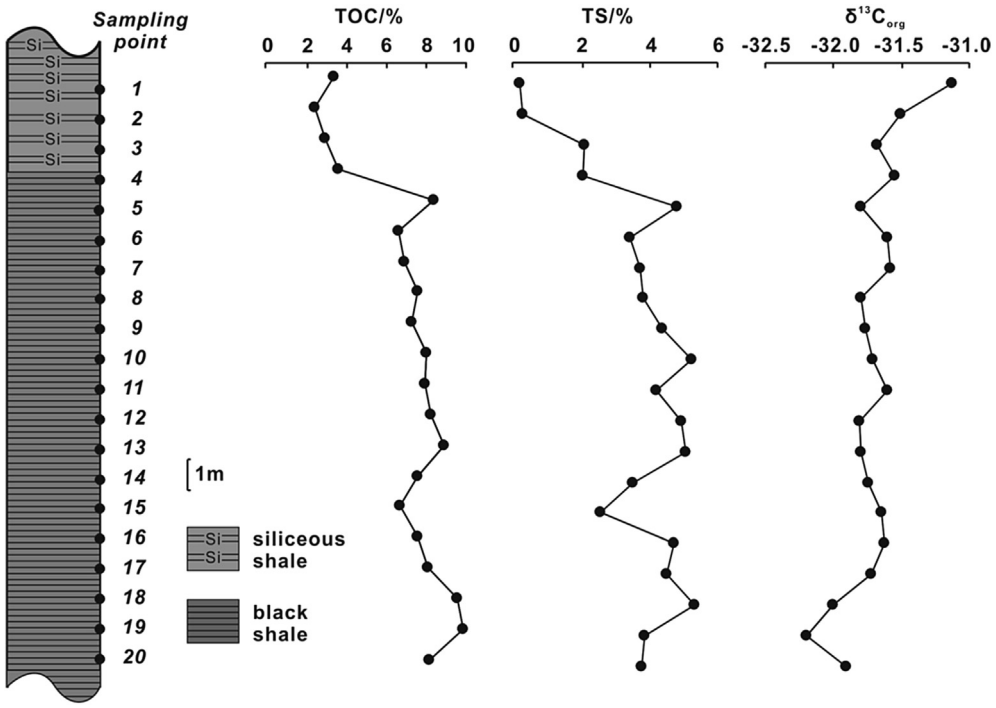

Fig. 2. Sampling information and stratigraphic profiles of Youyang section TOC and TS content and carbon isotope value of organic matter.

recent organisms should be evaluated (Brocks et al., 2008; Sherman et al., 2007). This has been minimized during sampling and analysis in this study. At highly mature stages, the organic geochemistry of sediments tends to be homogeneous and the primary geochemical differences may be difficult to determine, especially for biomarker's maturity index. In previous studies (Tuo et al., 2016), we investigated the distribution characteristics of biomarkers in the over-mature Lower Paleozoic shales in Sichuan Basin. The distribution characteristics of biomarkers in the three over-mature and regionally developed black shales (the Lower Cambrian, Upper Ordovician, and Lower Silurian) were significantly different, indicating the different of source material and organic characteristics. Geochemical significance of biomarkers in over-mature Cambrian black shales has been also reported in several recent studies (Jin et al., 2014; Han et al., 2015). Thus, the use of organic geochemistry to indicate the organic matter type of the Lower Cambrian Niutitang shale is considered to be reliable in this study.

Parameters extracted from GC-MS analysis are listed in Table 1. It is clear to see that *n*-alkanes are the dominant chemical components of saturated hydrocarbons in our samples. The carbon numbers of *n*-alkanes range from C_{14} to C_{27}, with a strong dominance of short-chain components (Fig. 3a). The distribution characteristics of terpenoids is shown in Fig. 3b. Both tricyclic terpanes and hopanes are abundant in all of the Lower Cambrian Niutitang shale. The major isoprenoid alkanes were pristane (Pr) and phytane (Ph), with Pr/Ph ratios ranging from 0.85 to 1.78. The ratios of Pr/*n*-C_{17} and Ph/*n*-C_{18} are shown in Fig. 4. The Pr/*n*-C_{17} ratios range from 1.08 to 8.52. The Ph/*n*-C_{18} ratios range from 0.6 to 3.62. The regular steranes are dominated by C_{27} steranes and the average relative abundance of C_{27}, C_{28} and C_{29} steranes is approximately 40.64%, 21.87%, and 37.49%, respectively.

4.4. Trace elements paleo-redox proxies

Several trace elements, including Mo, Re, U, and V, have been considered as indicators of redox conditions in paleo-depositional environments (Pratt and Davis, 1992; Crusius et al., 1996; Dean et al., 1997; Rimmer et al., 2004). Some trace element abundance ratios, such as V/(V + Ni), V/Cr, Ni/Co, U/Th (Jones and Manning, 1994; Hatch and Leventhal, 1992), have been used for restoring the redox conditions of a depositional environment. The Lower Cambrian Niutitang shales have V/(V + Ni) ratios ranging between 0.64 and 0.93, with an average value of 0.80; V/Cr ratio between 1.7 and 13.0, with an average value of 6.7; Ni/Co ratio between 2.81 and 10.7, with an average value of 6.5; U/Th ratio ranges between 1.31 and 9.86, with an average value of 5.82 (Table 2; Fig. 5). The Lower Cambrian Niutitang shales are considerably enriched in Mo (Table 2; Fig. 6), ranging between 39.8 and 149.7 ppm, with an average value of 97.2 ppm.

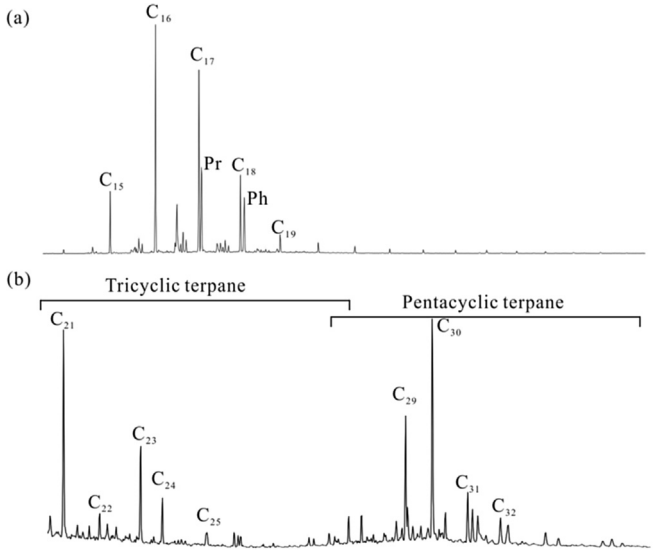

Fig. 3. Representative m/z 85 and m/z 191 mass chromatograms of saturated hydrocarbons. (a) m/z 85 mass chromatogram; (b) m/z 191 mass chromatogram.

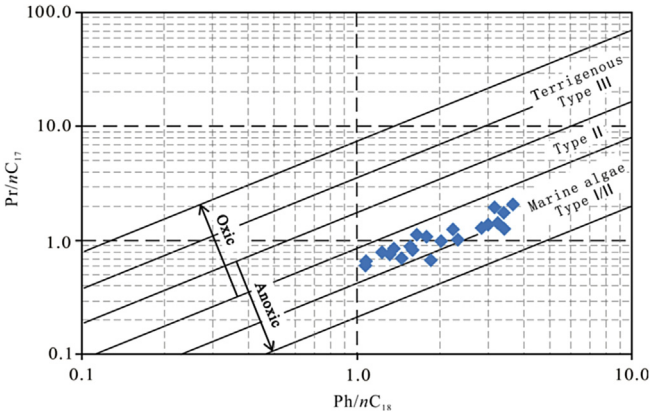

Fig. 4. Pristane, phytane composition of Niutitang shale in the study area.

between −39.6 and −30.4‰, with an average value of −36.1‰; the $\delta^{13}C_2$ values range between −39.6‰ and −18.6‰, with an average value of −29.7‰; the $\delta^{13}C_3$ values for the three samples range between −24.5‰ and −14.6‰.

5. Discussion

5.1. Organic matter types

Previous studies have conducted numerous investigations on the degree of thermal evolution of the Lower Cambrian shales in the Sichuan Basin and have found that the Lower Cambrian shales have reached the over-mature stage (Zou and Dong, 2010; Wang et al., 2010; Huang et al., 2012). Vitrinite reflectance (*Ro*) values are generally over 2.5% throughout the Sichuan Basin and are as high as 3.0 in the study area (Xie et al., 2013; Xiao et al., 2015). Rock-Eval pyrolysis is the primary method used to classify organic matter types. The type of organic matter is commonly characterized via a pyrolysis index, such as HI-OI (HI, hydrogen index; OI, oxygen index), H/C-O/C, S_2-TOC (S_2, remaining hydrocarbon potential), or T_{max}-HI. However, these pyrolysis indices cannot effectively evaluate organic matter types that are highly or overly thermally mature. The carbon isotope values of organic matter, which are primarily affected by the organic matter source and remain stable during the thermal evolution of the organic matter, can be used to evaluate the organic matter type. The $\delta^{13}C_{org}$ values of the Niutitang shales range between −32.4‰ and −31.1‰ (Table 1, Fig. 2). The average $\delta^{13}C_{org}$ values of the Lower Cambrian shales in the Upper Yangtze Platform is −31.9‰ (Liang et al., 2009), which is consistent with the results of this study. According to the evaluation standard presented by Hu and Huang (1991), sediments with $\delta^{13}C_{org}$ values lighter than −29.0‰ belong to type I organic matter. The $\delta^{13}C_{org}$ values of all Niutitang shale samples fall within this range, indicating type I organic matter with strong hydrocarbon generating capacity.

Biomarkers are widely used to reflect the source of organic matter in sediments. Low molecular weight *n*-alkanes (C_{15}-C_{19} *n*-alkanes) predominated, with *n*-C_{16} as the most abundant peak (therefore representing the main components) and with high $\sum C_{21}^{-}/\sum C_{22}^{+}$ values ranging from 7.5 to 138.4 (Table 1, Fig. 3a). These results indicate a major contribution of planktonic algae in the sedimentary organic matter. The studied shale samples exhibit

Table 2
Trace elements composition of the Niutitang shales from the Youyang section.

Sample no.	Trace elements (ppm)						V/(V + Ni)	V/Cr	Ni/Co	U/Th
	V	Cr	Ni	Mo	Th	U				
TL-3	694.2	134.4	93.5	53.2	2.95	5.46	0.88	5.2	4.31	1.85
TL-4	771.1	76.3	54.3	39.8	2.41	3.17	0.93	10.1	6.81	1.31
TL-5	337.3	116.0	86.1	106.0	1.90	13.58	0.80	2.9	2.81	7.13
TL-6	419.4	100.8	130.7	86.9	3.23	20.06	0.76	4.2	5.14	6.20
TL-7	1033.9	103.5	226.1	89.9	5.37	30.58	0.82	10.0	10.70	5.70
TL-8	756.6	105.5	183.1	81.9	5.60	44.03	0.81	7.2	6.67	7.86
TL-9	744.4	85.7	134.3	107.1	6.81	32.90	0.85	8.7	4.77	4.83
TL-10	482.6	90.7	127.1	116.4	3.69	25.69	0.79	5.3	5.21	6.97
TL-11	900.6	86.7	204.2	103.2	5.29	33.42	0.82	10.4	9.55	6.32
TL-12	482.7	65.7	120.6	94.4	5.63	32.07	0.80	7.3	4.72	5.70
TL-13	546.4	103.6	124.1	149.7	6.74	42.15	0.81	5.3	3.31	6.26
TL-14	1292.9	99.8	226.6	119.3	5.62	29.76	0.85	13.0	9.53	5.30
TL-15	340.9	205.5	188.0	93.6	5.62	19.49	0.64	1.7	8.58	3.47
TL-16	498.2	98.5	118.1	87.7	6.88	27.43	0.81	5.1	3.95	3.99
TL-17	424.0	102.8	196.6	110.7	5.65	55.78	0.68	4.1	10.14	9.86
TL-18	558.1	62.2	127.2	99.1	5.13	40.87	0.81	9.0	4.53	7.96
TL-20	460.5	95.2	168.9	114.2	4.21	34.86	0.73	4.8	9.81	8.29

4.5. Minerals

The mineralogical compositions of the selected nine shale samples are listed in Table 3. With an average value of 8%, pyrite ranges between 3% and 12%, and is positively correlated with TOC (Fig. 7). These samples are characterized with high quartz content in the range of 52–69%, and show a positive correlation between TOC and quartz contents (Fig. 8). The quartz content of the studied shales in Youyang profile is very similar with the results of Rongxi and Jinggang Niutitang shales (Tan et al., 2014). The quartz-related minerals are relatively high in the Lower Cambrian shales. The clay contents of the nine samples range between 9% and 29%, with an average value of 18%, and illite is the dominant mineral in all samples. The clay content is relatively low in the studied organic-rich Niutitang shales, which is consistent with previous research results of the Lower Cambrian shales in other areas in Southeastern Chongqing (Tan et al., 2014). An obviously negative linear correlation was observed between the total clay and TOC contents (Fig. 8). The average content of feldspar is approximately 10% with a range between 6% and 18%.

4.6. Geochemical characteristics of residual gas in shales

Carbon isotopic compositions of residual gases are listed in Table 4. Methane was recovered from all samples; ethane from 16 samples; propane only from three samples. The $\delta^{13}C_1$ values range

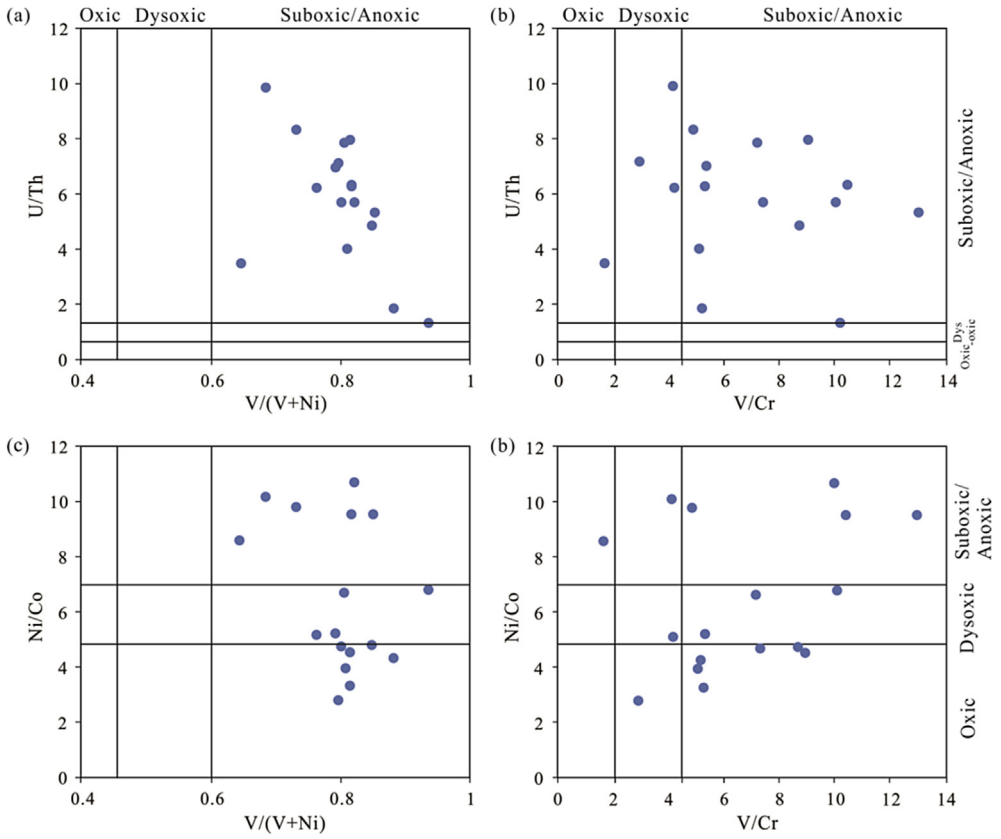

Fig. 5. Crossplots of trace-element ratios as paleoredox proxies. (a) U/Th vs. V/(V + Ni); (b) U/Th vs. V/Cr; (c) Ni/Co vs. V/(V + Ni); (d) Ni/Co vs. V/Cr.

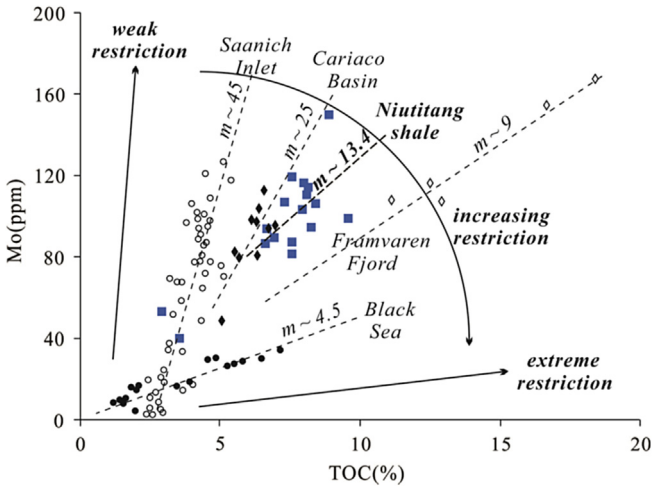

Fig. 6. Mo content versus TOC for Niutitang shale and Recent sediments of modern anoxic silled basins. Regression-line slopes (m in units of 10^{-4}): Saanich Inlet (hollow circle), m ~ 45 ± 5; Cariaco Basin (black diamond), m ~ 25 ± 5; Framavaren Fjord (hollow diamond): m ~ 9 ± 2; Black Sea (black circle): m ~ 4.5 ± 1. Above date modified from Algeo and Lyons 2006. Blue square represent Niutitang shale in Youyang section, m ~ 13.4 ± 5. (For interpretation of the references to colour in this figure legend, the reader is referred to the web version of this article.)

typical straight-chain *n*-alkanes distribution characteristics, indicating that the organic matter was sourced from autochthonous phytoplankton (Koopmans et al., 1999) and was in the thermal evolution range of the high maturity or post-mature gas-generating stage. The distribution patterns of terpenoids indicate the enrichment of tricyclic terpanes (Fig. 3b). The average value of ∑tricyclic terpanes/∑hopanes is 0.97, with relative higher abundance of tricyclic terpanes to hopanes in some samples. Tricyclic terpanes are widely distributed in crude oils and source rocks of marine or lacustrine origin and are considered to be diagenetic products of prokaryote membranes (Ourisson et al., 1982) and primitive bacteria (Grandville, 1982; Grantham, 1986). C_{27}, C_{28}, and $C_{29}\alpha\alpha\alpha$ (20R) steranes have an asymmetrical distribution in the shape of a "V", with a predominance of C_{29} steranes (Table 1). The distribution of biological markers in the studied shale samples suggests that organic matter was mainly derived from lower aquatic organisms and algae.

Isoprenoid alkanes in the sediment can also be used to estimate organic matter type. The result of a correlation study between Pr/nC_{17} and Ph/nC_{18} is consistent with that of the organic carbon isotope study, suggesting type I organic matter was deposited in strongly reducing marine conditions (Fig. 4). The carbon isotope values of the organic matter and distributions of biomarkers suggest that the organic matter type of the Niutitang shales is oil-prone and sapropelic (I), which has a strong oil generation capability.

5.2. Sedimentary environment

5.2.1. Constraints from organic geochemistry

The Lower Cambrian Niutitang shale is a super-rich source rock, with a total organic carbon content ranging from 2.42 to 9.89% in the Youyang profile (Fig. 2). The high TOC values indicate an anoxic setting lacking the bacteria that typically attack and destroy organic matter (Loucks and Ruppel, 2007). In an aerobic environment, bacteria thrive, and much of the organic material is consumed. Accordingly, the high abundance of organic matter in the Youyang profile indicates the sedimentary environment was generally

Table 3
TOC content and mineralogical composition of the Niutitang shales (%).

Sample no.	TOC	Quartz	Dolomite	Anorthose	Pyrite	Microcline	Total clays
TL-3	2.92	60	nd	6	3	2	29
TL-4	3.59	58	nd	7	7	2	25
TL-5	8.42	59	nd	9	11	1	20
TL-7	6.92	61	5	9	6	1	18
TL-11	7.95	64	4	9	7	2	14
TL-13	8.92	61	6	9	10	2	12
TL-16	7.58	52	5	15	9	3	17
TL-18	9.58	68	2	7	12	2	9
TL-19	9.89	69	nd	7	9	1	14

nd: no detected; Total Clays = illite + montmorillonite + chlorite.

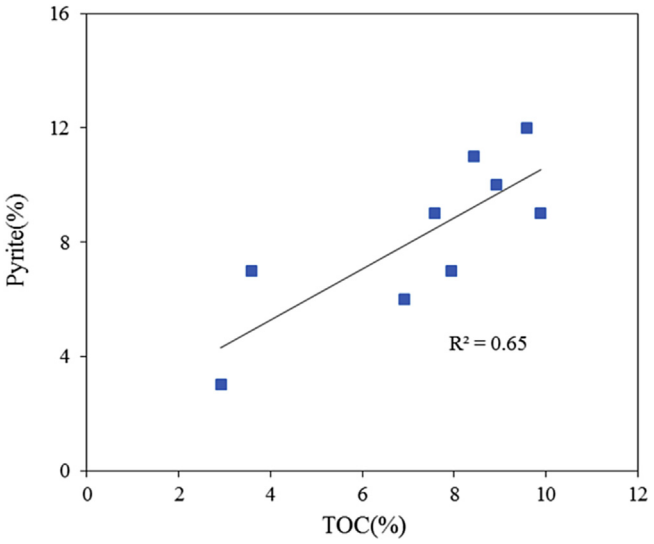

Fig. 7. Crossplots of TOC abundance versus pyrite.

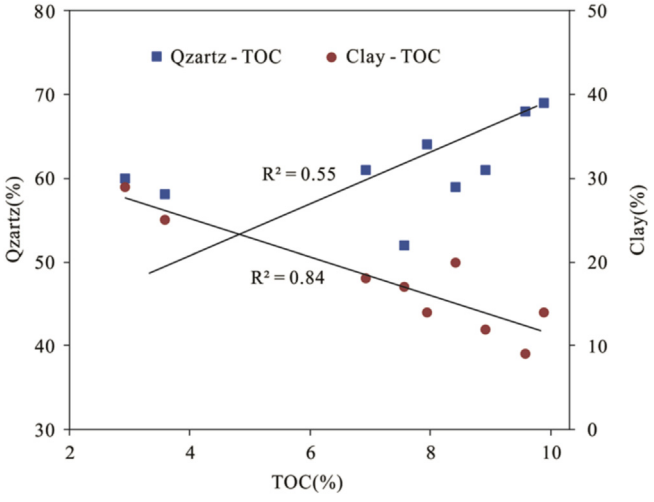

Fig. 8. Crossplots of TOC abundance versus quartz and clay.

anoxic during deposition of the Lower Cambrian Niutitang shales. The total sulfur (TS) content exhibits similar trends as TOC in the longitudinal direction and is similarly high in the lower part of the section. The total sulfur content ranges from 0.15 to 5.3%, with an average of 3.6%. The total sulfur content is susceptible to be disruption in an oxidizing environment. Thus, the high sulfur content suggests that the organic matter in well preserved, with

Table 4
Carbon isotopic characteristics of residual shale gas.

Sample no.	$\delta^{13}C_{org}$/‰	$\delta^{13}C_1$/‰	$\delta^{13}C_2$/‰	$\delta^{13}C_3$/‰	C_1/C_{2+}
TL-1	−31.1	−37.5	nd	nd	–
TL-2	−31.5	−39.4	nd	nd	–
TL-3	−31.7	−35.5	nd	nd	–
TL-4	−31.6	−38.4	−29.8	−14.6	48.09
TL-5	−31.8	−35.4	−18.6	−15.3	26.48
TL-6	−31.6	−35.8	−31.1	−24.5	12.96
TL-7	−31.6	−38.0	−30.4	nd	19.01
TL-8	−31.8	−36.5	−30.7	nd	34.19
TL-9	−31.8	−34.3	nd	nd	–
TL-10	−31.7	−35.3	−29.9	nd	28.86
TL-11	−31.6	−35.0	−29.2	nd	35.87
TL-12	−31.8	−39.6	−32.8	nd	29.01
TL-13	−31.8	−33.8	nd	nd	–
TL-14	−31.7	−36.7	nd	nd	–
TL-15	−31.7	−30.4	nd	nd	–
TL-16	−31.6	−35.3	−28.3	nd	61.93
TL-17	−31.7	−34.1	−29.0	nd	57.66
TL-18	−32.0	−34.7	−30.3	nd	29.82
TL-19	−32.2	−39.2	−32.7	nd	31.32
TL-20	−31.9	−36.7	−33.1	nd	30.84

nd: no detected.

little disturbance. In addition, the total sulfur content is positively correlated with TOC (Fig. 2), suggesting that the organic matter was well preserved after burial.

Previous studies have suggested that variations in the carbon isotopic composition of marine organic matter can be used for environmental interpretations (Arthur et al., 1985; Dean et al., 1986). The depositional environment can be well defined by organic carbon isotopic results (Freudenthal et al., 2001; Lehmann et al., 2002). The wide distribution of the anoxic environment will have an effect on the organic carbon isotopic value. The low $\delta^{13}C_{org}$ value can be explained by the anoxic conditions of the sedimentary environment. The Niutitang shales present a distinct trend of ^{13}C enrichment. The $\delta^{13}C_{org}$ values of the Niutitang shales range from −32.4‰ to −31.1‰, with an average of −31.8‰, significantly lighter than the value of modern euxinic environment sediments (e.g., the Black Sea, approximately −24‰; Freeman et al., 1994). A global anoxic event can result in a large number of biological extinctions and rapidly increase organic matter burial in sediment. Due to the preferential enrichment of ^{12}C, a large amount of organic matter rich in ^{12}C was buried and deposited (Wang et al., 2002). An anoxic environment can promote the formation of organic-rich intervals and enhance negative $\delta^{13}C_{org}$ excursions (Wang et al., 2015). In this study, the $\delta^{13}C_{org}$ values of the Niutitang Formation negatively correlated with TOC content (Fig. 2).

5.2.2. Constraints from trace element enrichment and redox indices

The trace element content of sediment can be influenced by many factors, including redox conditions, sediment accumulation

rates, diagenesis and later mineralization processes (Pratt and Davis, 1992). Molybdenum (Mo), uranium (U), and vanadium (V) are considered to be redox-sensitive (Pratt and Davis, 1992; Dean et al., 1997). Redox indices, including U/Th, V/Cr, V/(V + Ni), and Ni/Co, have been widely used to estimate the redox properties of ancient sedimentary environments (Hatch and Leventhal, 1992; Jones and Manning, 1994). Trace elements of the Lower Cambrian organic-rich black shales in the Yangtze Block have been studied extensively to reveal the paleosedimentary environment (Guo et al., 2007; Li et al., 2015; Wang et al., 2015).

High U/Th ratios are consistent with highly reducing conditions, with U/Th > 1.25 representing suboxic/anoxic environments and U/Th < 0.75 representing normal oxic marine sedimentary environments. The U/Th ratios in all the studied samples exhibit significant U enrichment relative to the ratio of PAAS (0.31, McLennan, 1989) and black shale (3.30, Calvert and Pedersen, 1993). The observed U/Th value is greater than 1.25, with an average of 5.82. V/(V + Ni) > 0.54 and V/Cr > 4.25 both represent anoxic environments. The measured V/(V + Ni) and V/Cr ratios agree with the U/Th result. In the Niutitang shale, the V/(V + Ni) ratio ranges between 0.64 and 0.93, with an average of 0.80, and the V/Cr ratio ranges between 1.7 and 13.0, with an average of 6.7 (Table 2). In the diagrams of U/Th vs. V/(V + Ni) and U/Th vs. V/Cr, most studied samples fall in the anoxic region (Fig. 5a, b), indicating that the Niutitang shale were deposited in an anoxic environment. The analysis result of the Ni/Co study is not perfectly in agreement with that of U/Th, V/(V + Ni), and V/Cr, but most samples plot in the dysoxic and anoxic regions (Fig. 5c, d).

Previous research suggests that sediments deposited from euxinic water are enriched in molybdenum (Brumsack and Gieskes, 1983; Koide et al., 1986; Brumsack, 1989). Thus, the Mo content has been used as an indicator of anoxic conditions and considered to be the best diagnostic element for sediment deposition under sulfate-reducing conditions (Dean et al., 1997). In the Well W201, the Mo contents of the Lower Cambrian Qiongzhusi black shales range from 16.9 to 72.7 ppm, with an average of 35.2 ppm. In the Well N206, Mo contents of the Qiongzhusi black shales range from 57.7 to 402.0 ppm, with an average of 154.0 ppm (Wang et al., 2015). The Mo content of the Niutitang shale ranges from 39.8 to 149.7 ppm, with an average of 97.2 ppm, which is significantly higher than the average value in normal sediment (2.6 ppm, Wedepohl, 1971) and black shales (10 ppm, Vine and Tourtelot, 1970). The Mo enrichment positively correlates with TOC content, indicating a strong coupling between Mo and TOC in the Niutitang shale, as shown in Fig. 6. Organic matter is the primary host phase for Mo in these Lower Palaeozoic shales, a finding that is supported by the strong correlation between the Mo and TOC concentrations. The Mo content versus TOC plot shows a comparison between the Niutitang shale and modern anoxic marine systems described by previous studies. The Niutitang shale falls in the restriction area and the average regression-line slope (Mo/TOC) is 13.4×10^{-4}, close to that of the Cariaco Basin (25×10^{-4}) and Framavaren Fjord (9×10^{-4}). The Mo-TOC diagram demonstrates that the redox conditions of the Niutitang Formation were anoxic and favourable for organic matter accumulation. The Mo-TOC relationships reveal that the Qiongzhusi Formation black shales were probably deposited under moderately restricted conditions.

5.2.3. Constraints from mineral enrichment

Pyrite is one of the important characteristic minerals in marine organic-rich sediments. The pyrite content and speciation in source rocks can be used to restore the redox state of the bottom water and to assess the paleosedimentary environment. The formation of pyrite is generally related to bacterial sulfate reduction. Under a hypoxic paleoaquifer environment, sulfate is reduced to H_2S and reduced sulfur using organic matter as a reducer and energy source. The reaction products further react with active iron to form a series of iron sulfides, eventually forming pyrite, which is preserved in the sediment (Leventhal et al., 1983). High pyrite contents reflect stable sedimentary water and high-salinity water compared with normal seawater. The water environment below the oxidation-reduction interface was saline and strongly reducing, which was favourable to the preservation of planktonic organic matter (Qin et al., 2010). The pyrite content of the Niutitang shale ranges from 3 to 12% and is positively correlated with TOC (Fig. 7).

Quartz, a major mineral in sedimentary rocks, has long been considered to be derived from the continental crust due to its chemically and mechanically resistant nature (Potter et al., 1980). The quartz content of marine sediments has been used to determine the distance to the shoreline (Blatt and Totten, 1981). Schieber et al. (2000) analyzed quartz silt from Late Devonian black shales in the New Albany Basin, eastern USA, using backscattered electron and cathodoluminescence imaging (BSE and SEM-CL). Schieber proposed that the majority of the quartz silt in the Late Devonian black shales did not originate from the continental crust. Quartz silt originally precipitated via diagenesis in algal cysts and other pore spaces, and the silica was derived from the dissolution of opaline skeletons of planktonic organisms, such as radiolaria and diatoms. Hence, in marine sediments, the use of quartz as a proxy for detrital input must be performed with caution. Biogenic quartz has been reported in an extensive study of North American black shales (Turgeon and Brumsack, 2006; Ross and Bustin, 2006; Chalmers et al., 2012).

The bulk mineralogy of the Lower Cambrian Niutitang black shale is dominated by quartz, accounting for 52–69% of the bulk rock (Table 3). Study of the ancient geography suggests that, during the Niutitang Age in the Early Cambrian, the study area was mainly a restricted deep shelf (Tenger et al., 2007). In this deep shelf sedimentary environment, terrigenous clastics were not deposited in significant amounts due to the long transport distance from the material source, associated with the deep sedimentary environment and long distance from the coast. Terrigenous contribution accounts for only a small portion of the quartz minerals. In addition, the quartz content of the Niutitang black shales positively correlated with the total organic carbon content (Fig. 8), which is similar to Devonian gas shales in Horn River Basin, Canada (Chalmers et al., 2012). With increasing quartz content, the biological accumulation amount and organic matter abundance in the sediments increased, indicating that biogenic quartz is an important source of the quartz content. In the Sichuan Basin, this positive correlation between quartz and TOC was also reported in previous studies of the Lower Silurian Longmaxi black shales (Nie and Zhang, 2012; Wang et al., 2014b). Detrital, authigenic, and biogenic quartz constitute the total quartz mineral of the organic-rich Niutitang shale. The quantitative evaluation of quartz mineral of different origin in the over-mature Lower Cambrian shales needs more intensive study in the future research. The clay content in the Niutitang Formation ranges from 9 to 29% (Table 3), with an average of 18%. An obvious reverse negative linear correlation between clay content and total organic carbon exists (Fig. 8), indicating that the terrigenous mineral input can significantly dilute the organic matter enrichment.

5.3. Formation mechanism of shale gas

The residual hydrocarbon index (S_2, I_H, bitumen A) of the oil-prone organic-rich Niutitang shale is extremely low. All studied shale samples show low pyrolysis S_2 peaks, with an average of 0.022 mg of hydrocarbons per gram of rock (Table 1). In some samples, the concentrations are below detection limits, and pyrolysis S_2 peaks cannot be determined. The relationship between S_2

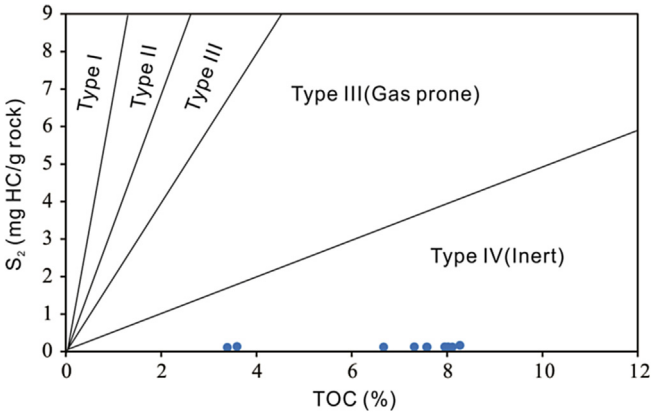

Fig. 9. Display of remaining hydrocarbon potential (S_2) versus total organic carbon (TOC) for the Niutitang Formation shale samples.

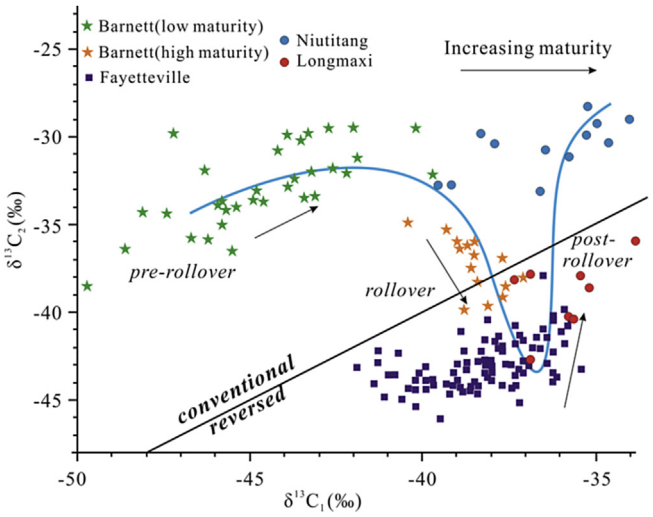

Fig. 10. Plot showing $\delta^{13}C_1$ versus $\delta^{13}C_2$ (Figure modified after Tilley and Muehlenbachs, 2013). Data of Barnett and Fayetteville sourced from Rodriguez and Philp, 2010; Zumberge et al., 2012. Data of Longmaxi shale in Sichuan Basin sourced from Dai et al., 2014.

and total organic carbon (TOC) in the Niutitang Formation shale samples indicates the existence of type IV inert solid bitumen (Fig. 9). The bitumen A values of the studied shale samples range from 6 to 34 ppm (Table 1). The hydrogen index (I_H) values are also very low, with the highest value not exceed 3 mg HC/g TOC. Additionally, limited amounts of soluble organic matter were detected in the studied samples, ranging from 7 to 19 ppm. The residual hydrocarbon index of the organic-rich Niutitang shales in Rongxi profile displays similar characteristics, with low S_2 (0.33–0.37 mg HC/g rock) and HI values (4–5 mg HC/g TOC) (Tan et al., 2015). The oil-prone Niutitang shale with a high abundance of organic matter but low residual hydrocarbon index values indicates that most of the hydrocarbons generated during the oil generation window were consumed during a stage of relatively high thermal evolution. The shale gas in the over-mature Niutitang Formation was mostly generated during secondary cracking processes.

The residual gases are the gases that are retained on the surfaces of the source rock pores. The geochemical characteristics of these gases reflect those of the shale gases. Previous studies (Shi et al., 2012) showed that the residual gases are composed mainly of hydrocarbon gas and carbon dioxide, with the hydrocarbon gas accounting for more than 80%. These gases can be measured reliably to obtain $\delta^{13}C_1$–$\delta^{13}C_3$ data. The results of the carbon isotope analyses satisfy the need for the geochemical study and application of residual gases. The residual gases in the Longmaxi shale have already been studied (e.g., Tang et al., 2015), but the gases in the Niutitang shale have not.

The $\delta^{13}C_1$ and $\delta^{13}C_2$ values of the Niutitang, Barnett (low maturity and high maturity), and Fayetteville shale gases are plotted in Fig. 10. The first inflection point on the curve was considered to be the beginning of secondary cracking and mixing of primary and secondary cracking gas (Tilley and Muehlenbachs, 2013; Rodriguez and Philp, 2010; Zumberge et al., 2012; Dai et al., 2014). The low-maturity Barnett shale gas plotted in the pre-rollover area, with a conventional $\delta^{13}C_1$–$\delta^{13}C_2$ trend ($\delta^{13}C_1 < \delta^{13}C_2$). As maturity increases, the $\delta^{13}C_2$ values of Barnett shale gas become increasingly negative and fall in the rollover area. As maturity continues to increase, a reversed $\delta^{13}C_1$–$\delta^{13}C_2$ trend ($\delta^{13}C_1 > \delta^{13}C_2$) occurs, and all highly over-mature Fayetteville shale gas exhibit this characteristic. As maturity increases still further, the $\delta^{13}C_1$–$\delta^{13}C_2$ trend becomes conventional again (Xia et al., 2013). The Niutitang shale falls in the post-rollover stage at a significantly high maturity with a conventional $\delta^{13}C_1$–$\delta^{13}C_2$ trend (Fig. 10). Unlike the Longmaxi shale gas in the Sichuan Basin, which plots in region III with a reversed $\delta^{13}C_1$–$\delta^{13}C_2$ trend (Dai et al., 2014), the even higher maturity Niutitang shale gas plots in region IV, in which the $\delta^{13}C_1$–$\delta^{13}C_2$ trend becomes conventional again. This pattern suggests that cracking of residual bitumen and wet gas at a high thermal maturity was the main source of the Niutitang residual gases and, therefore, the shale gas. This is also coincident with the observation that the Lower Cambrian shales have low amounts of soluble organic matter with large amounts of total organic matter.

In a comparative plot that shows the relationships between the carbon isotopic compositions of organic matter (OM‰), methane (C_1H_4‰), ethane (C_2H_6‰) and propane (C_3H_8‰, detected in three samples) in the residual gases (Fig. 11), all of the $\delta^{13}C_1$ values are lighter than those of OM, whereas most of the observed $\delta^{13}C_2$ values for the residual gases are heavier than those of OM in the corresponding samples. The ^{12}C-^{12}C bond is relatively easier to break than the ^{12}C-^{13}C and ^{13}C-^{13}C bonds (Rooney et al., 1995). The heavier isotopic value of ethane relative to OM suggests that the breaking down of wet gas under such high thermal maturity catagenesis involved the splitting of ethane bonds and the release of smaller (isotopically lighter) molecules, which likely led to the ^{13}C enrichment in the residual ethane (Tian et al., 2010). This finding further confirms that the shale gas stored in reservoirs in

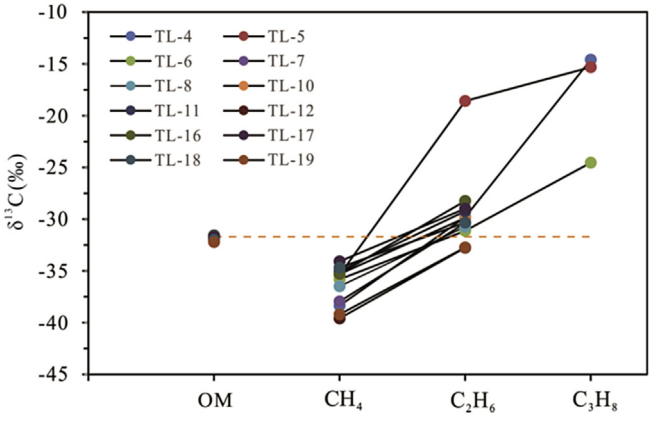

Fig. 11. $\delta^{13}C$ value of OM (organic matter), CH_4, C_2H_6, and C_3H_8.

these types of shale is mostly generated from the cracking of residual bitumen and wet gas during a stage of relatively high thermal maturity.

6. Conclusions

Based on our study of the organic matter characteristics, trace elements, mineral component, and residual shale gas carbon isotope distributions in the Lower Cambrian Niutitang black shale from southeastern Chongqing, the following conclusions can be drawn:

(1) Black and organic-rich shales in the lower part of the Lower Cambrian Niutitang Formation have TOC content ranging between 2.42% and 9.89% in the studied area. Stable carbon isotopes and biomarkers both indicate that the organic matter in the Niutitang black shales was mainly derived from both lower aquatic organisms and algaes and belong to type I kerogen.

(2) The trace elemental redox indices (U/Th, V/Cr, V/(V + Ni), Ni/Co) suggest that the Lower Cambrian organic-rich Niutitang shales were deposited in an anoxic environment and that the organic matter was well preserved after burial. The Mo-TOC relationships reveal that the redox conditions of the Niutitang Formation were anoxic and favourable for organic matter accumulation. The TOC content is positively correlated with quartz and pyrite but negatively correlated with clay content, indicating a strongly reducing sedimentary environment far from the coast of a continent.

(3) The residual gases in shales recovered with crushing method show a normal trend in the values of $\delta^{13}C_1$ and $\delta^{13}C_2$ and fall in post-rollover stage of very high thermal maturity. This normal tend in methane and ethane carbon isotopes, along with the extremely heavy $\delta^{13}C_2$ values as compared to those of their parent organic matter, indicates the shale gases were formed through the cracking of residual bitumen after oil expulsion and even the wet gas at a very high thermal maturity levels.

Acknowledgement

This research was supported by the National Programs for Fundamental Research and Development of China (973 Program) (Grant No.2012CB214701), CAS “Light of West China” Program, and the Key Laboratory Project of Gansu Province (Grant No.1309RTSA041). We thank two anonymous reviewers who refereed this paper and the Associate Editor Hui Tian for all their valuable comments that helped to greatly improve the quality of the paper.

References

Algeo, T., Lyons, T., 2006. Mo-total organic carbon covariation in modern anoxic marine environments: implications for analysis of paleoredox and paleohydrographic conditions. Paleoceanography 21, PA1016. http://dx.doi.org/10.1029/2004PA001112.

Arthur, M., Dean, W., Pratt, L., 1985. Geochemical and climatic effects of increased marine organic carbon burial at the Cenomanian/Turonian boundary. Nature 335, 714–717.

Blatt, H., Totten, M., 1981. Detrital quartz as an indicator of distance from shore in marine mudrocks. J. Sediment. Res. 51, 1259–1266.

Brocks, J.J., Grosjean, E., Logan, G.A., 2008. Assessing biomarker syngeneity using branched alkanes with quaternary carbon (BAQCs) and other plastic contaminants. Geochim. Cosmochim. Acta 72, 871–888.

Brumsack, H., Gieskes, J., 1983. Interstitial water trace-metal chemistry of laminated sediments from the Gulf of California, Mexico. Mar. Chem. 14, 89–106.

Brumsack, H., 1989. Geochemistry of recent TOC-rich sediments from the Gulf of California and the Black Sea. Geol. Rundsch. 78, 851–882.

Calvert, S., Pedersen, T., 1993. Geochemistry of recent oxic and anoxic marine sediments: implications for the geological record. Mar. Geol 113, 67–88.

Chalmers, G., Ross, D., Bustin, R., 2012. Geological controls on matrix permeability of Devonian Gas Shales in the Horn River and Liard Basins, northeastern British Columbia, Canada. Int. J. Coal Geol. 103, 120–131.

Chen, L., Lu, Y., Jiang, S., Li, J., Guo, T., Luo, C., Xing, F., 2015. Sequence stratigraphy and its application in marine shale gas exploration: a case study of the Lower Silurian Longmaxi Formation in the Jiaoshiba shale gas field and its adjacent area in southeast Sichuan Basin, SW China. J. Nat. Gas Sci. Eng. 27, 410–423.

Coplen, T., Brand, W., Geher, M., Groening, M., Meijer, H., Toman, B., Verkouteren, R., 2006. New guidelines for ^{13}C measurements. Anal. Chem. 787, 2439–2441.

Crusius, J., Calvert, S., Pedersen, T., Sage, D., 1996. Rhenium and molybdenum enrichments in sediments as indicators of oxic, suboxic and sulfidic conditions of deposition. Earth Planet. Sci. Lett. 145, 65–78.

Dai, J., Zou, C., Liao, S., Dong, D., Ni, Y., Huang, J., Wu, W., Gong, D., Huang, S., Hu, G., 2014. Geochemistry of the extremely high thermal maturity Longmaxi shale gas, southern Sichuan Basin. Org. Geochem. 74, 3–12.

Dean, W., Arthur, M., Claypool, G., 1986. Depletion of ^{13}C in Cretaceous marine organic matter: source, diagenetic, or environmental signal? Mar. Geol. 70, 119–157.

Dean, W., Gardner, J., Piper, D., 1997. Inorganic geochemical indicators of glacial–interglacial changes in productivity and anoxia on the California continental margin. Geochim. Cosmochim. Acta 61, 4507–4518.

Freeman, K., Wakeham, S., Hayes, J., 1994. Predictive isotopic biogeochemistry: hydrocarbons from anoxic marine basins. Org. Geochem. 21, 629–644.

Freudenthal, T., Wagner, T., Wenzhöfer, F., Zabel, M., Wefer, G., 2001. Early diagenesis of organic matter from sediments of the eastern subtropical atlantic: evidence from stable nitrogen and carbon isotopes. Geochim. Cosmochim. Acta 65, 1795–1808.

Grandville, B., 1982. Appraisal and development of a structural and stratigraphic trap oil field with reservoir in glacial to periglacial clastics. In: Halbouty, M.T. (Ed.), The deliberate search for the subtle trap. AAPG memoir 32. American Association of Petroleum Geologists, Tulsa, pp. 267–286.

Grantham, P., 1986. The occurrence of unusual C27 and C29sterane predominance in two types of Oman crude oil. Org. Geochem 9, 1–10.

Guo, T., Zhang, H., 2014. Formation and enrichment mode of Jiaoshiba shale gas field, Sichuan Basin. Petrol. Explor. Dev. 41, 31–40.

Guo, Q., Shields, G., Liu, C., Strauss, H., Zhu, M., Pi, D., Goldberg, T., Yang, X., 2007. Trace element chemostratigraphy of two Ediacaran-Cambrian successions in South China: implications for organosedimentary metal enrichment and silicification in the early Cambrian. Palaeogeogr. Palaeoclimatol. Palaeoecol. 254, 194–216.

Han, S., Hu, K., Cao, J., Pan, J., Xia, F., Wu, W., 2015. Origin of early Cambrian black-shale-hosted barite deposits in South China: mineralogical and geochemical studies. J. Asian Earth Sci. 106, 79–94.

Hao, F., Zhou, H., Lu, Y., 2013. Mechanisms of shale gas storage: implications for shale gas exploration in China. AAPG Bull. 97, 1325–1346.

Hatch, J., Leventhal, J., 1992. Relationship between inferred red-ox potential of the depositional environment and geochemistry of the Upper Pennsylvanian (Missourian) Stark Shale Member of the Dennis Limestone, Wabaunsee County, Kansas, U.S.A. Chem. Geol. 99, 65–82.

Hu, J., Huang, D., 1991. The Foundation of China Continental Petroleum Geology Theory. Petrol. Ind. Press, p. 189.

Huang, J., Zou, C., Li, J., Dong, D., Wang, S., Wang, S., Cheng, K., 2012. Shale gas generation and potential of the Lower Cambrian Qiongzhusi Formation in the Southern Sichuan Basin, China. Petrol. Explor. Dev. 39, 75–81.

Jarvie, D., Hill, R., Ruble, T., Pollastro, R., 2007. Unconventional shale-gas systems: the Mississippian Barnett Shale of north central Texas as one model for thermogenic shale-gas assessment. AAPG Bull. 91, 475–499.

Jin, X., Pan, C., Yu, S., Li, E., Wang, J., Fu, X., Qin, J., Xie, Z., Zheng, P., Wang, L., Chen, J., Tan, Y., 2014. Organic geochemistry of marine source rocks and pyrobitumen-containing reservoir rocks of the Sichuan Basin and neighbouring areas, SW China. Mar. Pet. Geol. 56, 147–165.

Jones, B., Manning, A., 1994. Comparison of geochemical indices used for the interpretation of palaeoredox conditions in ancient mudstones. Chem. Geol. 111–129.

Koide, M., Hodge, V., Yang, J., Stallard, M., Goldberg, E., Calhoun, J., Bertine, K., 1986. Some comparative marine chemistries of rhenium, gold, silver and molybdenum. Appl. Geochem. 1, 705–714.

Koopmans, M., Rijpstra, W., Klapwijk, M., de Leeuw, J., Lewan, M., Sinninghe Damsté, J., 1999. A thermal and chemical degradation approach to decipher pristine and phytane precursors in sedimentary organic matter. Org. Geochem 30, 1089–1104.

Lehmann, M., Bernasconi, S., Barbieri, A., McKenzie, J., 2002. Preservation of organic matter and alteration of its carbon and nitrogen isotope composition during simulated and in situ early sedimentary diagenesis. Geochim. Cosmochim. Acta 66, 3573–3584.

Leventhal, J., 1983. An interpretation of carbon and sulfur relationships in Black Sea sediments as indicators of environments of deposition. Geochim. Cosmochim. Acta 47, 133–137.

Li, Y., Fan, T., Zhang, J., Zhang, J., Wei, X., Hu, X., Zeng, W., Fu, W., 2015. Geochemical changes in the Early Cambrian interval of the Yangtze Platform, South China: implications for hydrothermal influences and paleocean redox conditions. J. Asian Earth Sci. 109, 100–123.

Liang, D., Guo, T., Chen, J., Bian, L., Zhao, Z., 2009. Some progresses on studies of hydrocarbon generation and accumulation in marine sedimentary regions,

southern China (Part 2): geochemical characteristics of four suites of regional marine source rocks, South China. Mar. Orig. Pet. Geol. 14, 1–15.
Loucks, R., Ruppel, S., 2007. Mississippian Barnett Shale: lithofacies and depositional setting of a deep-water shale-gas succession in the Fort Worth Basin, Texas. AAPG Bull. 91, 579–601.
McLennan, S., 1989. Rare earth elements in sedimentary rocks; influence of provenance and sedimentary processes. Rev. Miner. Geochem 21, 169–200.
Mei, M., Zhang, H., Meng, X., Chen, Y., 2006. Sequence stratigraphic division and framework of the Lower Cambrian in the Upper Yangtze region. Geol. China 33, 1292–1304.
Nie, H., Zhang, J., 2012. Shale gas accumulation conditions and gas content calculation: a case study of Sichuan Basin and its periphery in the Lower Paleozoic. Acta. Geol. Sin. Engl. 86, 349–361.
Ourisson, G., Albrecht, P., Rohmer, M., 1982. The microbial origin of fossil fules. Scientific Am 251, 44–51.
Peters, K., Walters, C., Moldowan, J., 2005. The Biomarker Guide: Interpreting Molecular Fossils in Petroleum and Ancient Sediments, second ed. Cambridge University Press, UK.
Potter, P., Maynard, J., Pryor, W., 1980. Sedimentology of Shale. Springer, New York.
Pratt, L., Davis, C., 1992. Intertwined fates of metals, sulfur and organic carbon in black shales. In: Pratt, L.M., Comer, J.B., Brassell, S.C. (Eds.), Geochemistry of Organic Matter in Sediments and Sedimentary Rocks, SEPM Short Course Notes, Soc. Sed. Geol., vol. 27, pp. 1–27.
Qin, J., Tao, G., Teng, G., Bian, L., Xie, X., Fu, X., 2010. Hydrocarbon-forming organisms in excellent marine source rocks in South China. Pet. Geol. Exper 32, 262–269.
Rimmer, S., Thompson, J., Goodnight, S., Robl, T., 2004. Multiple controls on the preservation of organic matter in Devonian-Mississippian marine black shales: geochemical and petrographic evidence. Palaeogeogr. Palaeoclimatol. 215, 125–154.
Rodriguez, N., Philp, R., 2010. Geochemical characterization of gases from the Mississippian Barnett Shale, Fort Worth Basin, Texas. AAPG Bull. 94, 1641–1656.
Rooney, M., Claypool, G., Chung, H., 1995. Modeling thermogenic gas generation using isotope ratios of natural gas hydrocarbons. Chem. Geol. 126, 219–232.
Ross, D., Bustin, R., 2006. Sediment geochemistry of the Lower Jurassic Gordondale Member, northeastern British Columbia. Bull. Can. Petrol. Geol. 54, 337–365.
Schieber, J., Krinsley, D., Riciputi, L., 2000. Diagenetic origin of quartz silt in mudstones and implications for silica cycling. Nature 406, 981–985.
Sherman, L., Waldbauer, J., Summons, R., 2007. Improved methods for isolating and validating indigenous biomarkers in Precambrian rocks. Org. Geochem. 38, 1987–2000.
Shi, B., Shen, P., Wang, X., Zhen, J., 2012. Groundbreaking gas source rock correlation research based on the application of a new experimental approach for adsorbed gas. Chin. Sci. Bull. 57, 4746–4752.
Tan, J., Horsfield, B., Mahlstedt, N., Zhang, J., Diprimio, R., Vu, T., Boreham, C., Van Graas, G., Tocher, B., 2013. Physical properties of petroleum formed during maturation of Lower Cambrian shale in the upper Yangtze Platform, South China, as inferred from PhaseKinetics modelling. Mar. Petrol. Geol. 48, 47–56. http://dx.doi.org/10.1016/j.marpetgeo.2013.07.013.
Tan, J., Horsfield, B., Fink, R., Krooss, B., Schulz, H., Rybacki, E., Zhang, J., Boreham, C., Van Graas, G., Tocher, B., 2014. Shale gas potential of the major marine shale formations in the Upper Yangtze Platform, South China, part III: mineralogical, lithofacial, petrophysical, and rock mechanical properties. Energy Fuels 28, 2322–2342. http://dx.doi.org/10.1021/ef4022703.
Tan, J., Horsfield, B., Mahlstedt, N., Zhang, J., Boreham, C., Hippler, D., Van Graas, G., Tocher, B., 2015. Natural gas potential of Neoproterozoic and lower Palaeozoic marine shales in the Upper Yangtze Platform, South China: geological and organic geochemical characterization. Int. Geol. Rev. 57 (3), 305–326.
Tang, Q., Zhang, M., Cao, C., Song, Z., Li, Z., Hu, X., 2015. The molecular and carbon isotopic constraints on origin and storage of Longmaxi Formation shale gas in Changning area, Sichuan Basin, China. Interpretation 3, SJ35–SJ47.
Tenger, G., Hu, K., Fang, C., Lv, J., Zhai, C., Zhang, C., 2007. High quality source rocks of lower combination in the Northern Upper-Yangtze area and their hydrocarbon potential. Nat. Gas Geosci. 18, 254–259.
Tian, H., Xiao, X., Wilkins, R., Gan, H., Guo, L., Yang, L., 2010. Genetic origins of marine gases in the Tazhong area of the Tarim basin, NW China: implications from the pyrolysis of marine kerogens and crude oil. Int. J. Coal Geol. 80, 17–26.
Tian, H., Pan, L., Xiao, X., Wilkins, R.W., Meng, Z., Huang, B., 2013. A preliminary study on the pore characterization of Lower Silurian black shales in the Chuandong Thrust Fold Belt, southwestern China using low pressure N_2 adsorption and FE-SEM methods. Mar. Petrol. Geol. 48, 8–19.
Tian, H., Pan, L., Zhang, T., Xiao, X., Meng, Z., Huang, B., 2015. Pore characterization of organic-rich Lower Cambrian shales in Qiannan depression of Guizhou Province, Southwestern China. Mar. Petrol. Geol. 62, 28–43.
Tilley, B., Muehlenbachs, K., 2013. Isotope reversals and universal stages and trends of gas maturation in sealed, self-contained petroleum systems. Chem. Geol. 339, 194–204.
Tuo, J., Wu, C., Zhang, M., 2016. Organic matter properties and shale gas potential of Paleozoic shales in Sichuan Basin, China. J. Nat. Gas Sci. Eng. 28, 434–446.
Turgeon, S., Brumsack, H., 2006. Anoxic vs dysoxic events reflected in sediment geochemistry during the Cenomanian-Turonian Boundary Event (Cretaceous) in the Umbria-Marche Basin of central Italy. Chem. Geol. 234, 321–339.
Vine, J., Tourtelot, E., 1970. Geochemistry of black shale deposits-a summary report. Econ. Geol. 65, 253–272.
Wang, C., Chen, X., Wang, X., 2002. Late Ordovician chemical anomaly and the environmental changes across the Ordovician-Silurian boundary in Yangtz Gorges. J. Stratigr. 26, 272–279.
Wang, F., Chen, J., Gao, G., Sun, Y., Peng, P., 2010. Reflectance of macroalgae-derived vitrinite-like macerals: an organic maturity indicator for pre-Devonian marine strata. Petrol. Explor. Dev. 37, 250–256.
Wang, S., Zou, C., Dong, D., Wang, Y., Huang, J., Guo, Z., 2014a. Biogenic silica of organic-rich shale in Sichuan Basin and its significance for Shale gas. Acta Sci. Nat. Univ. Pekin. 50, 476–486.
Wang, Y., Zhu, Y.M., Chen, S.B., et al., 2014b. Characteristics of the nanoscale pore structure in Northwestern Hunan shale gas reservoirs using field emission scanning electron microscopy, high-pressure mercury intrusion, and gas adsorption. Energy Fuels 28, 945–955.
Wang, S., Zou, C., Dong, D., Wang, Y., Li, X., Huang, J., 2015. Multiple controls on the paleoenvironment of the Early Cambrian marine black shales in the Sichuan Basin, SW China: geochemical and organic carbon isotopic evidence. Mar. Petrol. Geol. 66, 660–672.
Wedepohl, K.H., 1971. Environmental influences on the chemical composition of of shales and clays. Phys. Chem. Earth 8, 307–331.
Xia, X.Y., Chen, J., Braun, R., et al., 2013. Isotopic reversals with respect to maturity trends due to mixing of primary and secondary products in source rocks. Chem. Geol. 339, 205–212.
Xiao, X., Wei, Q., Gai, H., Li, T., Wang, M., Pan, L., Chen, J., Tian, H., 2015. Main controlling factors and enrichment area evaluation of shale gas of the Lower Paleozoic marine strata in south China. Petrol. Sci. 12, 573–586.
Xie, C., Zhang, J.C., Li, Y.X., et al., 2013. Characteristics and gas content of the Lower Cambrian dark shale in Well Yuke 1, Southeast Chongqing. Oil Gas Geol. 1, 004.
Zhang, J.C., Nie, H.K., Xu, B., et al., 2008. Geology conditions of shale gas accumulation in Sichuan Basin. Nat. Gas Ind. 28, 151–156.
Zhang, T.W., Yang, R.S., Milliken, K.L., et al., 2014. Chemical and isotopic composition of gases released by crush methods from organic rich mudrocks. Org. Geochem. 73, 16–28.
Zou, C.N., Dong, D.Z., 2010. Geological characteristics, formation mechanism and resource potential of shale gas in China. Petrol. Explor. Dev. 37, 641–653.
Zou, C.N., Yang, Z., Dai, J.X., et al., 2015. The characteristics and significance of conventional and unconventional Sinian–Silurian gas systems in the Sichuan Basin, central China. Mar. Petrol. Geol. 64, 386–402.
Zumberge, J., Ferworn, K., Brown, S., 2012. Isotopic reversal ('rollover') in shale gases produced from the Mississippian Barnett and Fayetteville formations. Mar. Petrol. Geol. 31, 43–52.